A dynamical model of a mobile inverted pendulum with linear and non linear controllers with time difference.

Ubaid Asif Farooqui[1], Dr. Chinta Mani Tiwari[2]

Department of Mathematics,Maharishi University of InformationTechnology,Lucknow.

uasif2u@gmail.com

Article Info
Page Number: 1044-1062
Publication Issue:
Vol. 71 No. 4 (2022)

Article History
Article Received: 25 March 2022
Revised: 30 April 2022
Accepted: 15 June 2022
Publication: 19 August 2022

Abstract: This study compares two linear controllers and a fuzzy logic controller (FLC) on a two-wheeled mobile inverted pendulum that is represented by system matrices with integrated time delay. By acting on the control input following a lookup, it contributes to energy conservation, making the system robust even when affected by the impacts of specially built system time delays. In this section, we look at three different performance indices: (i) the tilt angle's standard deviation; (ii) the root mean square of the signal sent to the electrical motors; and (iii) the convergence zone of the tilt angle. According to the experimental findings, the LQR with Kalman filter controller uses less energy and has a smaller standard deviation of error than the PID.This study compares the performance of two linear controllers and a fuzzy logic controller (FLC) on a two-wheeled mobile PID controller. The fuzzy controller, however, has a bigger convergence region. According to the performance measures, fuzzy control was shown to be the best way for controlling the time-delayed mobile inverted pendulum because it has a unique fuzzy granular preview control.

Key words: fuzzy logic, LQR, PID, granual computing, inverted pendulum.

1. INTRODUCTION:

In academia, the principles of system dynamics and feedback control are typically covered using mobile inverted pendulum robots, which are unstable mechanical systems with nonlinear dynamics similar to those of a traditional inverted pendulum [1]. These robots have also been used in a number of industries, such as agriculture, medicine, and transportation [3], [4], thanks to their autonomy, flexibility, and small size, which increases their usefulness in confined or hazardous working settings [5]. Generally speaking, these vehicles are affected by a variety of variables, including measurement noise, unmodeled dynamics, estimated parameter errors, and external perturbations [6]. The several control strategies available for these systems demand a thorough understanding of the mathematical model, which can be obtained using the Lagrange equations [1], [2], [7], [8], Newton-Euler equations [9], Gibbs-movement Appell's equations[3], [10], or Kane's method [1]. Due to the mechanism that uses a rotary servo to govern the pendulum over the upright equilibrium position, the rotary inverted pendulum has long been employed as a test bed in the control domain. This intricate dynamic plant then serves as a model for control education. The model can be developed into a helpful tool for different defence and military applications, and it has been used in the literature to map the logic applied to the control problem in the disciplines of humanoid robot walking, gesture control, segway transit, and satellite launch, among other areas. It is rare for the literature to examine a system that includes a time delay. For double and rotating inverted pendulum models, which is the plant under consideration here, Srikanth and Kumar [2, 5] constructed dynamic models. An technique to dealing with unpredictable time delays was put up by Daswon [6]. A state-dependent stabilisation criterion was put out by Sun et al. [7] and a method for deterministic time delay in control configuration was given by Benitez-Perez and Garcia-Nocetti [8]. being novel. The system has been used to map the logic applied to control problems in a variety of fields, including humanoid robot walking, gesture control, segway transportation, and satellite launch, among others. The idea being explored here is that previewing or looking up values is efficient since subsequent control actions are conducted, which is something that is not found in the literature and is being presented here. In their study [9], Tria et al. focus on the development of a fuzzy regulator for the active and reactive powers in order to explore the application of a variable control law to improve the dynamic behaviour of a wind turbine system utilising sliding mode control as the control strategy. Mohiuddin [10] Few studies assess the effectiveness of various control systems, despite the fact that the two-wheeled inverted pendulum has been the subject of extensive investigation. [1] analyses the three implemented controllers (FLC, LQR, and PID) on five different dimensions: (I) rising time (ii), (iii), settling time (iii), (iv) peak current supplied to the motors, and (v) linear displacement of the robot's platform collected before steady state (tilt angle near to zero). The robot was started with throughout the experiments with having a tilt angle of 24 degrees. [20] uses simulation to compare the rising time, settling time, overshoot, and steady state error of an FLC and a PID controller with respect to the linear position. The standard deviation of the tilt angle and the root mean square value of the control law, along with the zone of convergence of the initial tilt angle, are the two statistical metrics that the current article suggests employing to compare performance. This paper presents a novel, energy-efficient method for regulating the rotating inverted pendulum that makes use of a novel fuzzy preview controller. When compared to the real-time performance of a Quanser rotary inverted pendulum controlled with pole placement and fixed poles, the proposed model performs better in controlling peak overshoots and settling time specifications because it incorporates the time delay component into the system definition using row and column generation.

Required Mathematical Model to evaluate the performance:

Here we are going to introduce mathematical modeling for time delay of inverted pendulum a great work done by srikanth and kumar in 2017[1] on rotary inverted pendulum under time delays.The state model defined in Eqs. (3) and (4) is obtained from [2] K. Srikanth and G. V. N. Kumar, “Rotary inverted pendulum control and the impact of time delay on switching between stable and unstable states with enhanced particle swarm optimization,” International Journal of Computer and Communication System Engineering, vol. 2, no. 4, pp. 569-574, 2018.

Using the basic dynamic equations defined in Eqs. (1) and (2).

$$M_0\ddot{\theta}_0 + M_1\theta_1 \cos\theta_0\ddot{\theta}_1 - M_2 \sin\theta_0 \cos\theta_0\dot{\theta}_1^2 - M_3\, g\sin\theta_0 = 0, \tag{1}$$

$$M_1 \cos\theta_0\ddot{\theta}_1 + M_4 + (M_4 \sin^2\theta_0)\ddot{\theta}_1 - M_1 \sin\theta_0\ddot{\theta}_0^2 + 2M_2 \sin\theta_0 \cos\theta_0\dot{\theta}_0\dot{\theta}_1 = \tau \tag{2}$$

where τ in Eq. (2) refers to the control input which is applied to the shaft of the arm and M_i ($i = 0, 1, 2, 3, 4$) in Eqs. (1) and (2) are positive system parameters defined as

$$M_0 = I_1 + l_1^2 m_1 \tag{3}$$

$$M_1 = m_1 l_1 L_2 \tag{4}$$

$$M_2 = l_1^2 m_1 \tag{5}$$

$$M_3 = l_1 m_1 \tag{6}$$

$$M_4 = I_2 + l_2^2 m_2 + L_2^2 m_1 \tag{7}$$

The mathematical model for the rotary inverted pendulum is taken directly as in [2] which is an integrated model of the system with time delay given by the generic form of

$$\dot{X} = AX + BU \tag{8}$$

where X representing 5 states for the translation and rotation of the arm and the pendulum with 4 states that represent the system model by Eqs. (8) and (9). One additional state that represents the time delay is integrated into the system. The model is reconfigured with the delay embedded in order to make the system a minimum state variable model which makes the unified representation easier and decoupling the system into various canonical forms easier. The output equation is

$$Y = CX + DU \tag{9}$$

The fuzzy control block diagram model that is proposed is represented in figure1.

As shown in Figure1, the important parameters that are playing a key role are the error and the error rate which represent two inputs to the fuzzy preview controller which lookups the values based on which a decision is made and the output is passed on to the controller for amplification of the signal which is then passed as input to the plant. The feedback path has a LQR controller which does the state feedback control. The fuzzy granular based preview controller has a faster rule explosion which results in efficient control.

A weighted average method is adopted to calculate the hierarchical fuzzy controller with type-1 fuzzy controller and type-2 fuzzy controller.

$$u = w_{\text{type 1}} * u_{\text{type1fuzzy}} + w_{\text{type 2}} * u_{\text{type2fuzzy}} \quad (10)$$

As given in Eq. (10), where granulation is causing refinement in the way the control effort is used for the smoother control of the plant model. The incremental control action is not only a function of error and rate of error but also the time delay component which makes it a nonlinear controller which is more efficient than a liberalized LQR controller in terms of the control effort for reduced oscillations.

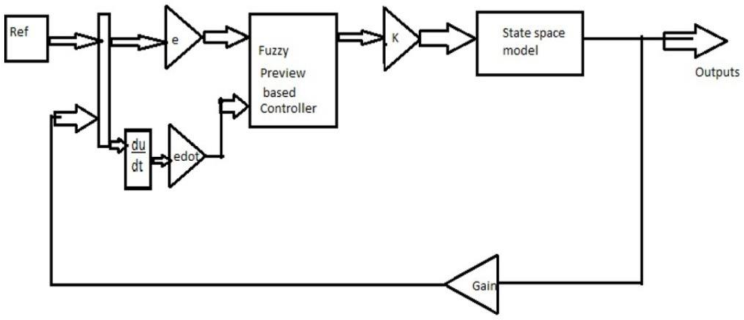

Figure 1

DYNAMIC MODELING:

This dynamical model is inspired by [3] chate and rengifo 2017(comparative analysis between fuzzy logic control, LQR control with kalman filter and PID control for a two wheel inverted pendulum.)

In Figure 2, a two-dimensional diagram of the mobile inverted pendulum robot is shown.

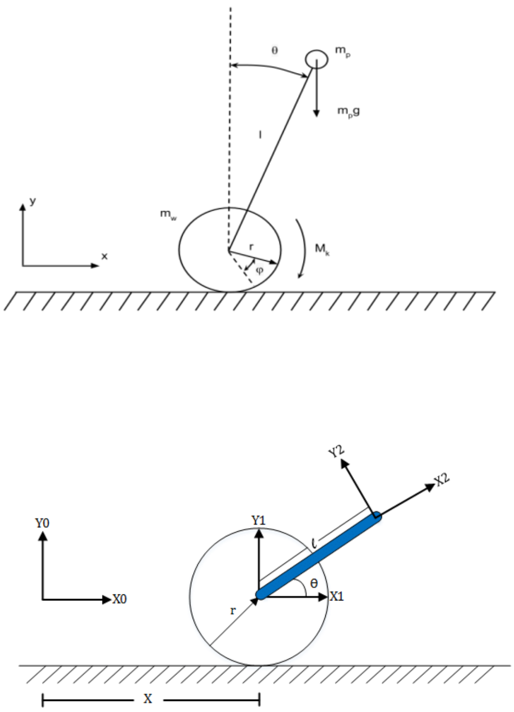

Figure:2 Diagram of the mobile inverted pendulum robot

The following table summarises the robot's parameters:

Parameter	Symbol	Value	Unit
Pendulum body length	L	0.08530	M
Wheel radius	R	0.03310	M
Wheel mass	M	0.05304	Kg
Pendulum mass	M	0.39277	Kg
Wheel inertia momentum	J_1	5.8111×10^{-5}	$Kg\ m^2$
Pendulum inertia momentum	J_2	3.1754×10^{-4}	$Kg\ m^2$
Gravity	G	9.8	m/s^2

An image of the two wheeled inverted pendulum InstaBot SRAT-2 is shown in Figure 3.

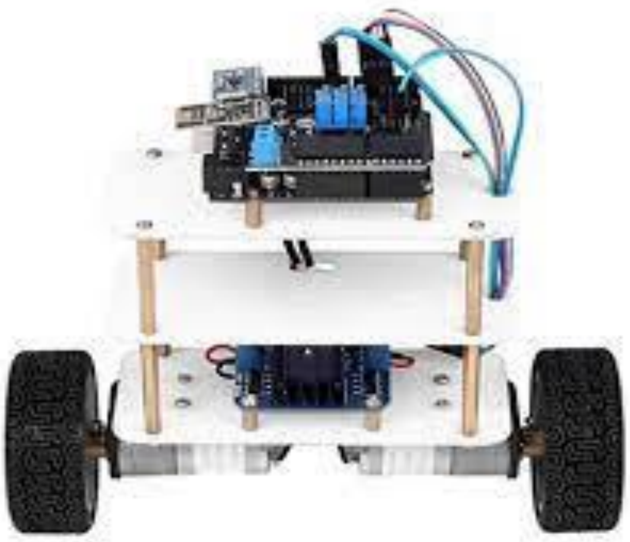

Figure 3: Front view of Mobile inverted pendulum InstaBot SRAT-2.

The following mathematical model is obtained using the Lagrange formalism:

$$\begin{bmatrix} M + m + \frac{j_1}{r^2} & -ml\sin\theta \\ -ml\sin\theta & ml^2 + j_2 \end{bmatrix} \begin{bmatrix} \ddot{x} \\ \ddot{\theta} \end{bmatrix} + \begin{bmatrix} -ml\dot{\theta}^2 & \cos\theta \\ & 0 \end{bmatrix} + \begin{bmatrix} & 0 & \\ -mgl & & \cos\theta \end{bmatrix} = \begin{bmatrix} \frac{1}{r} \\ 0 \end{bmatrix} \Gamma$$
(11)

Where

$$\begin{bmatrix} M + m + \frac{j_1}{r^2} & -ml\sin\theta \\ -ml\sin\theta & ml^2 + j_2 \end{bmatrix} = I(q)$$

$$\begin{bmatrix} \ddot{x} \\ \ddot{\theta} \end{bmatrix} = \ddot{q}$$

$$\begin{bmatrix} -ml\dot{\theta}^2 & \cos\theta \\ 0 & \end{bmatrix} = H(q, \dot{q})$$

$$\begin{bmatrix} 0 & \\ -mgl & \cos\theta \end{bmatrix} = G(q)$$

$$\begin{bmatrix} \frac{1}{r} \\ 0 \end{bmatrix} = E$$

$I(q)$ is the inertia matrix, $H(q, \dot{q})$ is the centrifugal and Coriolis forces vector, and $G(q)$ is thegravitational forces vector. Model (1) may be recast as a four-differential equation state-space model:

$$\dot{x} = \begin{bmatrix} \dot{x_1} \\ \dot{x_2} \\ \dot{x_3} \\ \dot{x_4} \end{bmatrix}, \; F = \begin{bmatrix} x_3 \\ x_4 \\ I^{-1}(x_2)\,(E\,\Gamma - H(x_2, x_4) - G(x_2)) \end{bmatrix} \qquad (12)$$

Where the state vector is defined as:

$$x_1 = x \quad x_2 = \theta - \frac{\pi}{2}$$
$$x_3 = \dot{x} \quad x_4 = \dot{\theta}$$

To design a linear controller, the model described by 2 must be first linearized at the equilibrium point defined by:

$$\begin{matrix} \bar{x}_1 = 0 & \bar{x}_2 = 0 \\ \bar{x}_3 = 0 & \bar{x}_4 = 0 \end{matrix} \qquad (13)$$

From the linearization process the following model is obtained:

$$\dot{x} = Ax + Bu \qquad (14)$$

$$A = \begin{bmatrix} 0 & 0 & 1 & 0 \\ 0 & 0 & 0 & 1 \\ 0 & -\frac{gl^2m^2r^2}{d_n} & 0 & 0 \\ 0 & -\frac{glmc_n}{d_n} & 0 & 0 \end{bmatrix}$$

$$B = \begin{bmatrix} 0 \\ 0 \\ \frac{r(ml^2 + J_2)}{d_n} \\ \frac{lmr}{d_n} \end{bmatrix}$$

$$c_n = J_1 + Mr^2 + mr^2$$
$$d_n = J_1J_2 + J_2Mr^2 + J_1l^2m + J_2mr^2 + Ml^2mr^2$$

PID Controller:

The tilt angle error is defined as the difference between the set point (0 degrees) and the observed tiltangle in this linear controller. The equation defines the control law (5)

$$u(t) = K_p\left(e(t) + \frac{1}{T_i}\int_0^t e(\tau)d\tau + T_d\frac{de(t)}{dt}\right) \qquad (15)$$

The following three terms comprise Equation (5): proportional, integral, and derivative. The proportionalaction is obtained by multiplying the gain value (K) by the error function. With a large value of K p, the steady state error decreases and the system responds more quickly to the defined set point, but it might also increase the output signal's oscillations [21]. By contrast, the integral action reduces steady state error by iteratively accumulating previous errors. Finally, the derivative action dampens the output oscillations caused by the proportional and integral actions. The derivative gain value improves the closed response's stability [21]. According to this, the optimal controller values were K p = 47:5, Ki = 0:05, and K d= 0:2.

Controller LQR:

The LQR controller is designed in accordance with (4)'s linear state space model, and the control law is defined as follows:

$$u = -Kx \qquad (16)$$

Where K is the gain of the state feedback and x denotes the state vector. The closed loop state-space model of the system is presented below using equation (6):

$$\dot{x} = (A - BK)x \qquad (17)$$

The LQR controller's objective is to locate each eigenvalue of the matrix A -BK in the left half plane s in such a way that the system's dynamic is stable and the quadratic cost function is minimised:

$$J = \frac{1}{2}\int_0^\infty x^T(t)Wx(t) + u^T(t)Ru(t)dt \qquad (18)$$

W is a 4 * 4 positive semidefinite matrix, while R is a positive scalar.

$$W = \begin{bmatrix} 1 & 0 & 0 & 0 \\ 0 & 190 & 0 & 0 \\ 0 & 0 & 1 & 0 \\ 0 & 0 & 0 & 0.7 \end{bmatrix}, R = 0.1$$

A position controller for the mobile inverted pendulum robot was implemented using the linear dynamic model (4) by altering the matrices W and R, which correspond to the system's states and inputs, respectively. The controller gain K obtained from such matrices is as follows:

$$K = [3.1623 \quad 44.1759 \quad 6.2140 \quad 0.3223]$$

Estimating the tilt angle using a Kalman Filter:

The mathematical technique by which the Kalman filter obtains the new state is based on a prediction and correction mechanism, in which gain compensation between the previous estimate and the current observation enables convergence to the system's real states. The suggested Kalman filter implementation combines the data from an accelerometer and a gyroscope. The accelerometer data is tied to angular orientation, whereas the gyroscope data is related to angular velocities. The following mathematical model is defined in light of this:

$$\begin{aligned} \dot{x} &= u \\ z &= x \end{aligned} \qquad (19)$$

Where u is the gyroscope reading, z is the accelerometer-calculated orientation, and x is the estimated tilt angle. The following Kalman equations derive from discretizing the continuous time fusion sensor model (9):

Prediction

$$\begin{aligned} \hat{x}_k^- &= \hat{x}_{k-1} + hu_k \\ \sigma_k^- &= \sigma_{k-1} + Q \end{aligned} \qquad (20)$$

Update

$$\begin{aligned} G_k &= \sigma_k^-(\sigma_k^- + \rho)^{-1} \\ \hat{x}_k &= \hat{x}_k^- + G_k\left(z_k - \hat{x}_k^-\right) \\ \sigma_k &= (1 - G_k)\sigma_k^- \end{aligned} \qquad (21)$$

this particular system, u_k is the angular velocity measured with the gyroscope, z_k is the orientation estimated from the measurements delivered by the accelerometer and $\hat{x}_k$ is the estimated orientation. The Kalman filter implementation was performed using the KalmanFilter [1] from TKJElectronics.

Fuzzy Control:

By introducing degrees of truth in a proposition and degrees of membership in a set as actual values in the range [0, 1], fuzzy logic provides an alternative to classical reasoning and set theory. This is done in orderto obtain a more realistic approximation of human reasoning.

The fuzzy PD controller developed for the robot InstaBot SRAT-2 takes the current value of the error signal (Error) and its temporal derivative as inputs (ErrorChange). We define three fuzzy sets for the variable (Error): Negative (N) error, Zero (Z) error, and Positive (P) error, as well as three fuzzy sets for the variable (ErrorChange): Negative Change (NC), Zero Change (ZC), and Positive Change (P) (PC).

We define four fuzzy sets for the control law: Large Negative (LN), Small Negative (SN), No Control

Law (NCL), Small Positive (SP), and Large Positive (LP), with No Control Law being a triangular set and the remaining sets being singletons. The developed fuzzy PD controller is built on a foundation of nine rules, as shown in Table 2.

	PC	ZC	NC
P	LP	SP	NCL
Z	SP	NCL	SN
N	NCL	SN	LN

Table 2: Rules matrix for the fuzzy PD controller

Figure 4 depicts a surface diagram of the control law derived by combining the aforementioned fuzzy setsand the rules listed in Table 2.

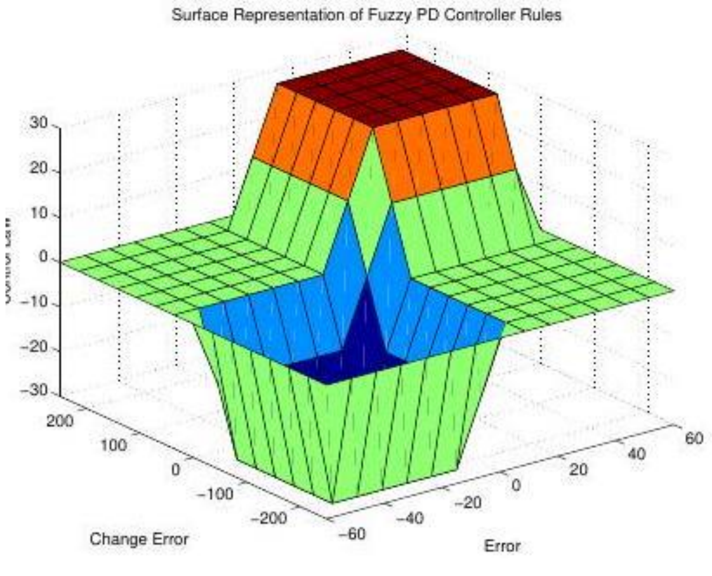

Figure 4: Fuzzy PD controller surface diagram applied to the robot InstaBot SRAT-2. Input variables: Error (axis x), Error Change (axis y), output variable: Control Law (axis Z)

IV. INDEXES OF PERFORMANCE:

The three controllers described in the previous section were compared using the following indices:

(1) The error's standard deviation:

$$\varepsilon_e = \sqrt{\frac{1}{N}\sum_{k=1}^{N} [\theta_d(k) - \theta(k)]^2} \qquad (22)$$

Being εe the standard deviation of the error signal, N the number of samples, θd(k)≜0 the desired tilt angle and θ(k) the measured tilt angle.

(2) The control law's root mean square:

$$\varepsilon_u = \sqrt{\frac{1}{N}\sum_{k=1}^{N} u^2(k)} \qquad (23)$$

Where εu is the root mean square value of the control effort u(k)

(3) The convergence region of the tilt angle was determined by initialising the robot at various angles of inclination and observing whether it falls or converges to the equilibrium position. Gradually increasing the initial tilt angle until the controllers were unable to restore to equilibrium/position = 0,

The first two indices were calculated many times (N=11) for each controller, each time using a different data set. The three controllers were compared using the average value of each index.

V RESULTS OF EXPERIMENTS

The figures 5 and 6 exhibit the outcomes gained from the implementation of each controller. The tilt angle as a function of time is depicted in Figure 4, and the control law is depicted in Figure 5.

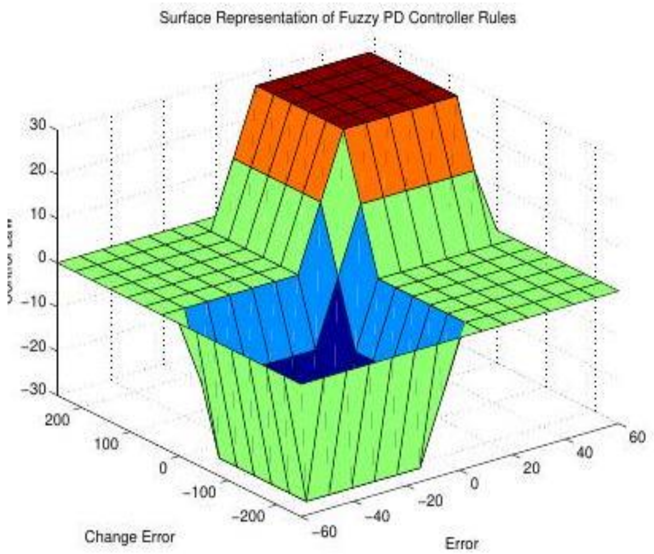

Figure 5

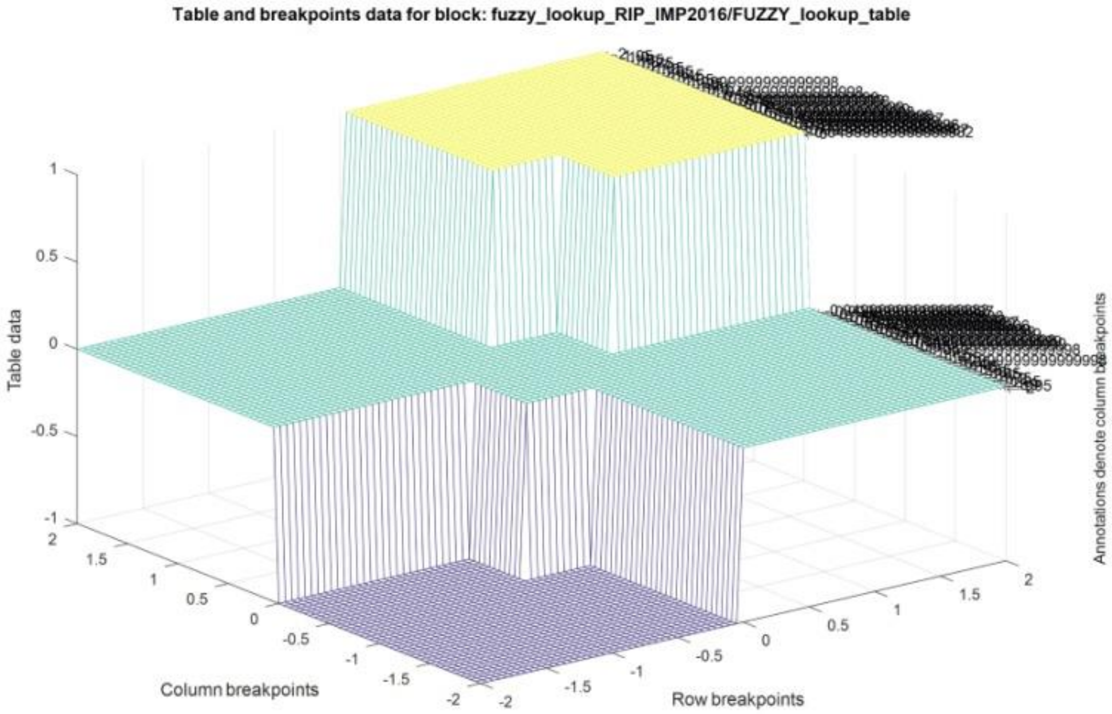

Figure 6

IV INDEXES OF PERFORMANCE:

The three controllers described in the previous section were compared using the following indices:

1. Standard deviation of the error

$$\varepsilon_e = \sqrt{\frac{1}{N}\sum_{k=1}^{N} [\theta_d(k) - \theta(k)]^2}$$

Being εe the standard deviation of the error signal, N the number of samples, $\theta d(k) \triangleq 0$ the desired tilt angle and $\theta(k)$ the measured tilt angle.

2. Root mean square of the control law

$$\varepsilon_u = \sqrt{\frac{1}{N}\sum_{k=1}^{N} u^2(k)}$$

3. The region of convergence of the tilt angle was obtained by initializing the robot with different degrees of inclination and determining whether it falls or it converges to the

equilibrium position. The initial tilt angle was gradually increased until the controllers were not able to return to the equilibrium position θ=0.

For each controller the first two indexes were calculated multiple times (N=11), each time using a different data set. The comparison between the three controllers was made by using the average value of each index.

RESULTS OF EXPERIMENTS:

The figures 5 and 6 exhibit the outcomes gained from the implementation of each controller under time delay. The tilt angle as a function of time is depicted in Figure 5, and the control law is depicted in Figure 6.

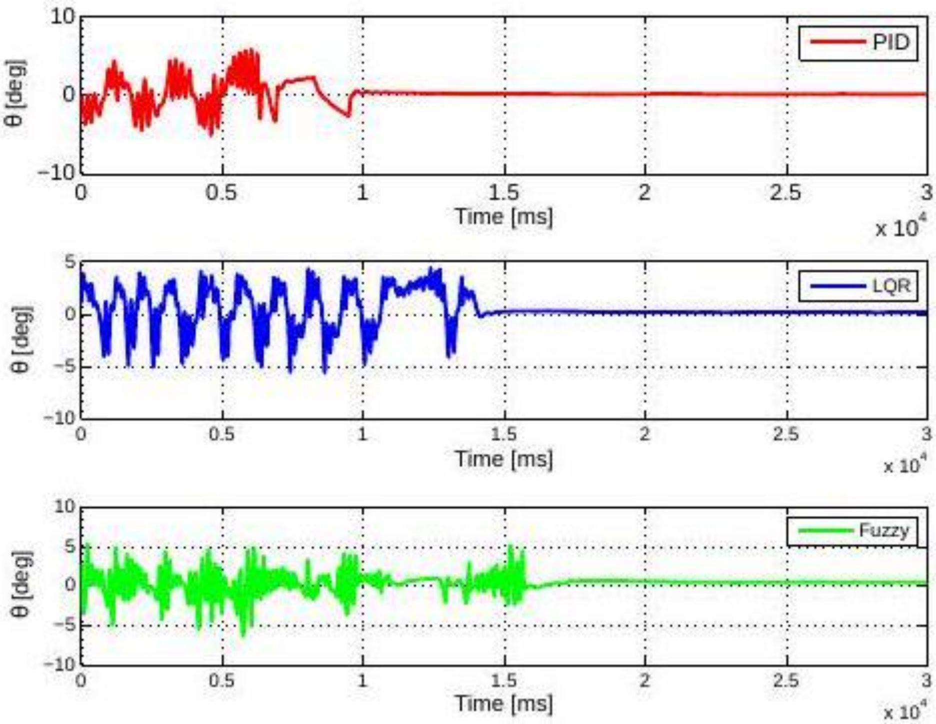

Figure 7: Time response of the implemented controllers (tilt angle) (i) PID , (ii) LQR with Kalman filter, (iii) fuzzy PD.

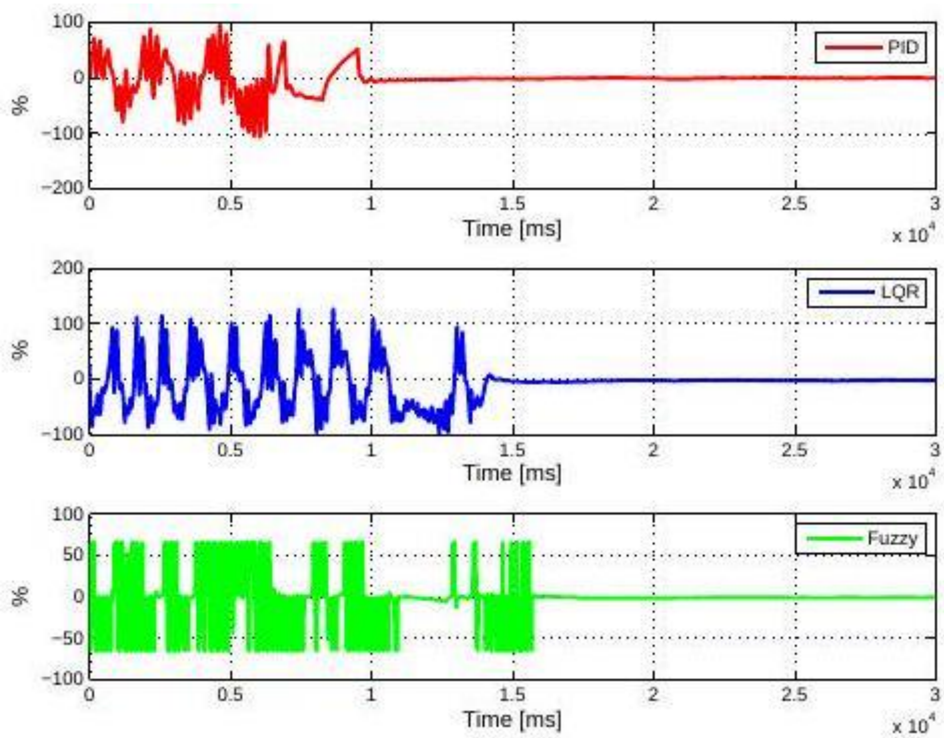

Figure 8: Control effort obtained from the implemented controllers (i) PID , (ii) LQR with Kalman filter, (iii) fuzzy PD.

Table 3 presents the average value of the performance indexes (εe and εu) obtained from the eleven test developed for each controller.

Controller	εe()	εu(%)
PID	1.95	37.7719
LQR	1.1559	26.4835
FuzZy	0.7689	12.4778

Table 3: Comparison of the average of standard deviations obtained from the eleven experiments realized with each controller.

Tables 4 and 5 show the ratios of the performance indexes of the linear controllers and the fuzzy control.

εePID/εeFuzzy	εeLQR/εeFuzzy	Least error
2.5361	1.5033	LQR

Table 4: Comparison of the ratios of standard deviations of error in the implemented controllers.

εuPID/εuFuzzy	εuLQR/εu Fuzzy	Least control effort
3.0271	2.1224	LQR

Table 5: Comparison of the ratios of standard deviations of control effort of the implemented controllers.

Figure 6 presents the critical convergence angles for the three implemented controllers. In the case of the PID controller, it has a poor performance due to the integral component which caused the control law to overact by the presence of a steady state error for a long period of time. LQR and fuzzy PD controllers did not present this inconvenience due to the absence of cumulative components in its control law.

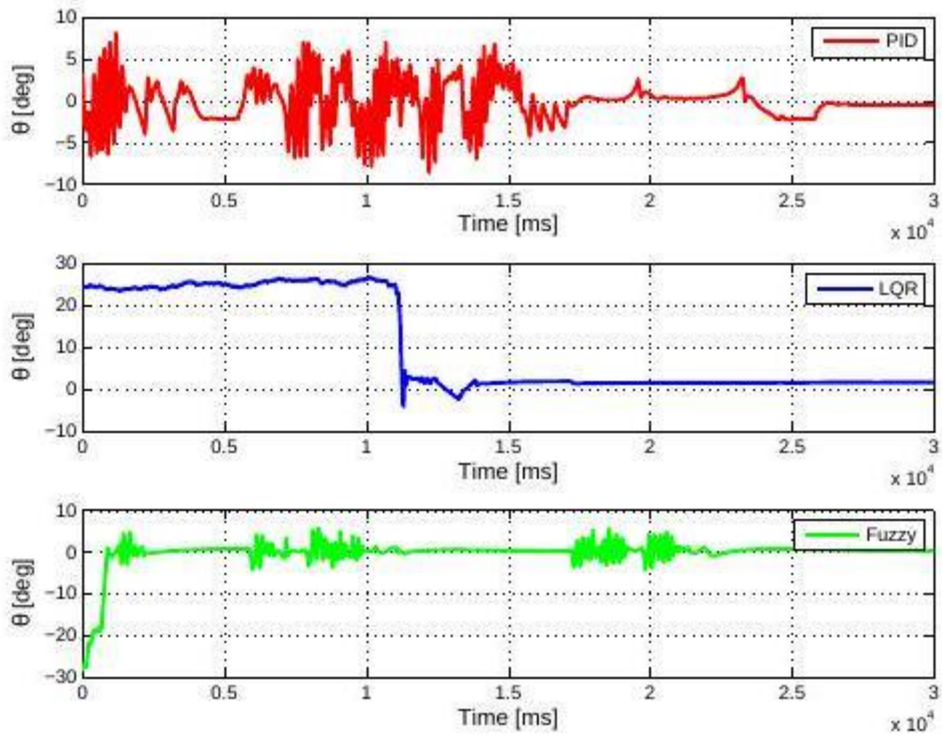

Figure 9: Critical convergence angle of the implemented controllers (i) PID (ii) LQR with Kalman filter, (iii) fuzzy PD.

Table 6 shows the range of initial tilt angles for which the control convergences to desired equilibrium point.

PID	LQR	Fuzzy	Most convergence region

[−4,4]	[−24.4,24.4]	[−28,25]	Fuzzy

Table 6: Comparison of the convergence regions found in the implemented controllers.

Figure 7 presents the trajectory of the robot in the phase plane (θ,θ) for an initial tilt angle close the critical angle of Table 6.

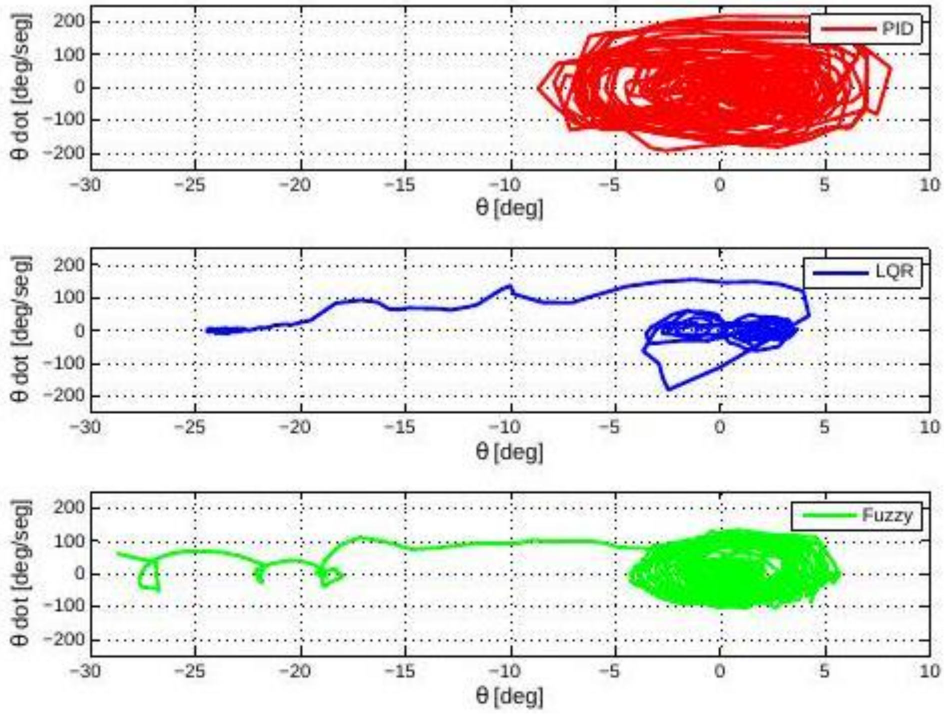

Figure 10: Convergence towards the equilibrium point ($\theta=0, \dot{\theta}=0$) of the implemented controllers (i) PID, (ii) LQR with Kalman filter, (iii) fuzzy PD.

It is observed that the PID convergence region is the smallest from the three implemented controllers, due to the control law overflow produced by the integral component. The LQR and fuzzy controllers present a wide range of initial values for which the controller can return to the desired set point.

Table below showing case for time delay

Test case of error variations.

Case ID	**E**	**Edot**	**Standard ref**	**Control action**
1	20	.002	.001	Success
2	2	.002	.001	Success
3	2	0.2	.001	Fails
4	2	.002	.001	Fails
5	2	.2	.001	Fails

Case ID	E	Edot	Standard ref	Control action
6	2	.02	1	Fails
7	2	.002	1	Success
8	.002	.002	1	Fails
9	.002	.00002	1	Fails
10	.002	.00002	.001	Fails
11	20	20	.001	Fails
12	2000	20	.001	Fails
13	2000	2000	1	Fails

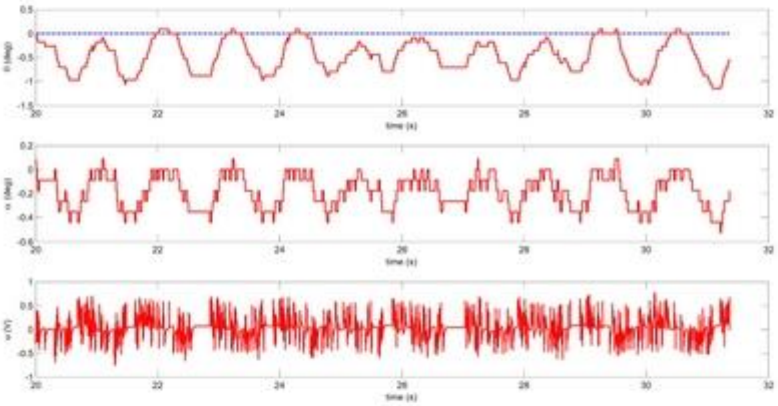

Figure 11: Typical real time performance of RIP with offset.

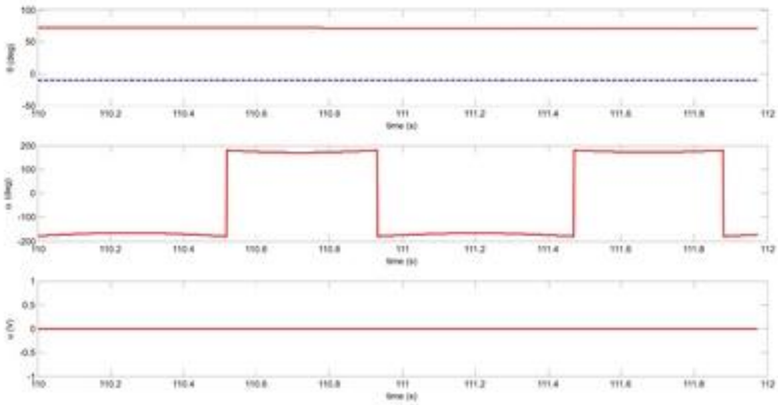

figure 12:Typical stabilization failure case in real time.

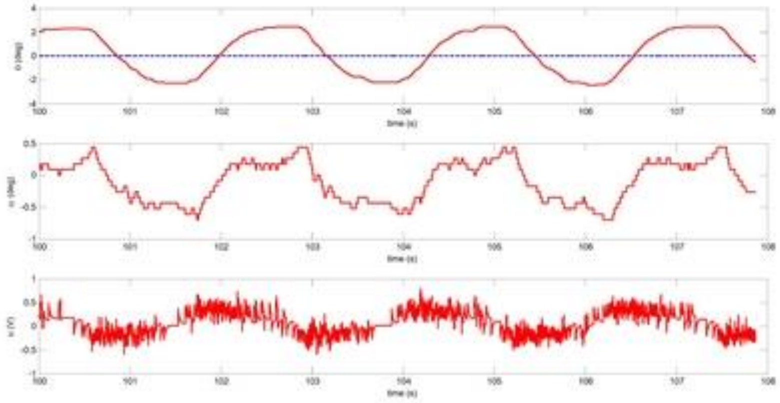

Figure 13:Swing up and stabilization in real time

The range of beginning tilt degrees for which the control converges to the desired equilibrium point is shown in Table 6.

Due to the integral component's control law overflow, the PID convergence zone is the smallest of the three implemented controllers. LQR and fuzzy controllers accept a broad range of beginning values before returning to the desired set point. The surface plot of the fuzzy lookup table is depicted in Figure. the rule explodes using the derivative of error as one of the two inputs. When contrasted to the situation of taking just the rule, the rule explosion is sped up by passing the two values. The outcome unequivocally demonstrates the viability of a solution using the created lookup definitions, which serve as the rule base. In Figures, the switching between stable and unstable zones for the laboratory model of the Quanser rotating inverted pendulum, a genuine experiment done on the test bed, can be shown clearly as the status of control for the system from swing up to upright equilibrium.

CONCLUSION:

This analysis with Lagrange formalism shows that the dynamical model of a mobile inverted pendulum robot preview-based fuzzy controller with granular computing can stabilize with three position in this article. Three controllers were implemented for this robot, two linear (PID and LQR) and one nonlinear (Fuzzy-PD). Three performance indices were used to compare the experimental outcomes achieved for each controller. Two of them, depending on the tilt angle's standard deviation and the control effort. The third index represents the range of initial tilt degrees that converge on the equilibrium point. The fuzzy controller was found to have a reduced error deviation and less energy consumption, as well as a larger zone of attraction to the equilibrium point, using these three metrics. The Kalman filter designwas used to improve the LQR controller's estimation of the robot orientation angle, resulting in a lower deviation error result, preview control is better than other methods is that it cuts down on the amount of time it takes to do the calculations when compared to the PID controller.

REFERENCES:

1. A. Bature, S. Buyamin, M. N. Ahmad, and M. Muhammad, "A comparison of controllers for ballancing two wheeled inverted pendulum robot," International Journal of

Mechanical & Mechatronic Engineering IJMME - IJENS, 2017.

2. Mahler and J. Haase, “Mathematical model and control strategy of a two-wheeled self-balancing robot,” in 39th Annual Conference of the IEEE Industrial Electronics Society, (IECON), Nov 2017, pp. 4198– 4203.
3. M. Azimi and H. Koofigar, “Model predictive control for a two wheeled self balancing robot,” in Proceeding of the lnternational Conference on Robotics and Mechatronics (RSIIISM), Tehran, Feb. 2017.
4. R . Brisilla and V. Sankaranarayanan, “Nonlinear control of mobile inverted pendulum,” Robotics and Autonomous Systems, vol. 70, pp. 145 – 155, 2018.
5. L . Sun and J. Gan, “Researching of two-wheeled self-balancing robot base on LQR combined with PID,” in Intelligent Systems and Applications (ISA), 2010 2nd International Workshop on, May 2015, pp.1–5.
6. G V. Raffo, M. G. Ortega, V. Madero, and F. R. Rubio, “Two-wheeled self-balanced pendulum workspace improvement via underactuated robust nonlinear control,” Control Engineering Practice, vol. 44, pp. 231 – 242, 2018.
7. O . Jamil, M. Jamil, Y. Ayaz, and K. Ahmad, “Modeling, control of a two-wheeled self-balancing robot,” in Robotics and Emerging Allied Technologies in Engineering (iCREATE), 2014 International Conference on, April 2014, pp. 191–199.
8. K . Peng, X. Ruan, and G. Zuo, “Dynamic model and balancing control for two-wheeled self-balancingmobile robot on the slopes,” in Proceedings of the 10th World Congress on Intelligent Control and
9. J Akeson, A. Blomdell, and R. Braun, “Design and control of yaip- an inverted pendulum on two wheels robot,” in Proceedings of the 2006 IEEE International Conference on Control Applications, Munich, Oct 2016.
10. F. Sun, Z. Yu, and H. Yang, “A design for two-wheeled self-balancing robot based on kalman filter and LQR,” in International Conference on Mechatronics and Control (ICMC), Jinzhou., Jul. 2014.
11. T.-J. Ren, T.-C. Chen, and C.-J. Chen, “Motion control for a twowheeled vehicle using a self-tuning PID controller,” Control Engineering Practice, vol. 16, no. 3, pp. 365 – 375, 2010.
12. C . Xu, M. Li, and F. Pan, “The system design and lqr control of a two-wheels self-balancing mobile robot,” in Electrical and Control Engineering (ICECE), 2011 International Conference on, Sept 2011, pp. 2786–2789.
13. W.-J. Wang and C.-H. Huang, “Model-based fuzzy control application to a self-balancing two- wheeled inverted pendulum,” in IEEE Control Applications, (CCA) and Intelligent Control, (ISIC),, July 2009, pp. 1158–1163.
14. Y -H. Wen, Y.-S. Lin, and Y.-G. Leu, “Design and implementation of the balance of two-wheeled robots,” in Advanced Robotics and Intelligent Systems (ARIS), 2013 International Conference on, May 2013, pp. 130– 134.
15. J Wu and W. Zhang, “Design of fuzzy logic controller for twowheeled self-balancing robot,” in Strategic Technology (IFOST), 2011 6th International Forum on, vol. 2, Aug 2011, pp. 1266–1270.
16. C.-H. Chiu, Y.-F. Peng, and Y.-W. Lin, “Intelligent backstepping control for wheeled

inverted pendulum," Expert Systems with Applications, vol. 38, no. 4, pp. 3364 – 3371, 2011.

17. C.-H. Chiu, Y.-W. Lin, and C.-H. Lin, "Real-time control of a wheeled inverted pendulum based on an intelligent model free controller," Mechatronics, vol. 21, no. 3, pp. 523 – 533, 2011.
18. C.-H. Chiu, W.-R. Tsai, M.-H. Chou, and Y.-F. Peng, "Two – wheeled robot control based on self- tuning output recurrent CMAC," in Proceedings of the International MultiConference of Engineers and Computer Scientists, vol. 1, Hong Kong, March 2009.
19. N . Nakpong and S. Yamamoto, "Just-in-time predictive control for a two-wheeled robot," in ICT and Knowledge Engineering (ICT Knowledge Engineering), 2012 10th International Conference on, Nov 2012, pp. 95–98.
20. A. N. K. Nasir, M. A. Ahmad, R. Ghazali, and N. S. Pakheri, "Performance comparison between fuzzy logic controller FLC and PID controller for a highly nonlinear two-wheels balancing robot," in First International Conference on Informatics and Computational Intelligence (ICI),, Dec 2011, pp. 176–181.
21. K . J. Astrom and T. Hagglund, Control PID avanzado. Pearson Prentice Hall, 2009.
22. S. Jadlovska and J. Sarnovsky, "Application of the state dependent Riccati equation method innonlinear control design for inverted pendulum systems," in Proceedings of the IEEE 11th International
23. Y. Zhang, X. Zhu, and Z. Huang, "Fuzzy sets based granular logics for granular computing," in Proceedings of International Conference on Computational Intelligence and Software Engineering,

    Wuhan, China, 2019, pp. 1-6. https://doi.org/10.1109/CISE.2009.5363975
24. A. Rubio-Solis, G. Panoutsos, and S. Thornton, "A datadriven fuzzy modelling framework for the classification of imbalanced data," in Proceedings of IEEE 8th International Conference on Intelligent Systems (IS), Sofia, Bulgaria, 2019, pp. 302-307. https://doi.org/10.1109/IS. 2016.7737438
25. S. Wang and W. Pedrycz, "Robust granular optimization: a structured approach for optimization under integrated uncertainty," IEEE Transactions on Fuzzy Systems, vol.23, no. 5, pp. 1372-1386, 2019. https://doi.org/10.1109/ TFUZZ.2014.2360941
26. A. Petrosino and S. K. Pal, "Guest editorial on decision making in human and machine vision," IEEE Transactions on Systems, Man, and Cybernetics: Systems, vol. 44, no.5, pp. 521-522, 2019.

    https://doi.org/10.1109/TSMC.2019. 2313155
27. W. Pedrycz, R. Al-Hmouz, A. Morfeq, and A. Balamash, "The design of free structure granular mappings: the use ofthe principle of justifiable granularity," IEEE Transactions on Cybernetics, vol. 43, no. 6, pp. 2105-2113, 2018. https: //doi.org/10.1109/TCYB.2013.2240384
28. K. Srikanth and G. V. N. Kumar, "Rotary inverted pendulum control and the impact of time delay on switching between stable and unstable states with enhanced particle swarm optimization," International Journal of Computer and Communication System Engineering, vol. 2, no. 4, pp. 569-574, 2018.